DOI:10.22337/2587-9618-2023-19-1-135-146

TIME ANALYSIS OF A CONSTRUCTIVELY NONLINEAR SYSTEM WITH ONE-WAY CONNECTIONS

Alexander N. Potapov, Nail T. Tazeev

South Ural State University, Chelyabinsk, RUSSIA

Annotation: An active method of suppressing wind auto-oscillations of an overground gas pipeline model is considered, which allows the system to be tuned from the resonant frequency by changing its design scheme with the help of a vibration damping device operating on the principle of one-way connection (OWC). A new mathematical model of vibrations with a symmetric form of natural vibrations of the system is proposed. Variants of vibration models with one and two OWC, located in the central span of the design scheme of the gas pipeline, are considered. The implementation of a non-stationary dynamic process is carried out within the framework of the theory of temporal analysis for a model of an overground gas pipeline in the form of a multi-span continuous beam with point masses located in the design sections of the model. The equation of motion is presented in the matrix form of the Duhamel integral, taking into account internal friction, which follows the disproportionate damping model. Computer simulation of the problem for a system with 39 degrees of freedom is carried out. The kinematic and force parameters of the dynamic response of the dissipative system are obtained, a comparative analysis of the proposed oscillation model for the design models with one and two OWC is given, and the efficiency of the model with two OWC is shown.

Keywords: overground gas pipeline, auto-oscillations, vibration damping device, connection, natural mode of vibration, stiffness matrix, displacement

ВРЕМЕННОЙ АНАЛИЗ КОНСТРУКТИВНО НЕЛИНЕЙНОЙ СИСТЕМЫ С ОДНОСТОРОННИМИ СВЯЗЯМИ

А.Н. Потапов, Н.Т. Тазеев

ФГАОУ ВО «Южно-Уральский государственный университет» (НИУ), г. Челябинск, РОССИЯ

Аннотация: Рассмотрен активный способ гашения ветровых автоколебаний модели надземного газопровода, позволяющий отстраивать систему от резонансной частоты путем изменения ее расчетной схемы с помощью устройства гашения колебаний, работающего по принципу односторонней связи (ОС). Предложена новая математическая модель колебаний с симметричной формой собственных колебаний системы. Рассмотрены варианты моделей колебаний с одной и двумя ОС, размещенными в центральном пролете расчетной схемы газопровода. Реализация нестационарного динамического процесса выполнена в рамках теории временного анализа для модели надземного газопровода в виде многопролетной неразрезной балки с точечными массами, расположенными в расчетных сечениях модели. Уравнение движения представлено в матричной форме интеграла Дюамеля с учетом внутреннего трения, подчиняющегося модели непропорционального демпфирования. Проведено компьютерное моделирование задачи для системы с 39 степенями свободы. Получены кинематические и силовые параметры динамической реакции диссипативной системы, дан сравнительный анализ предложенной модели колебаний для расчетных моделей с одной и двумя ОС и показана эффективность модели с двумя ОС.

Ключевые слова: надземный газопровод, автоколебания, устройство гашения колебаний, односторонняя связь, форма собственных колебаний, матрица жесткости, перемещение

INTRODUCTION

In operational practice overground gas pipelines, the phenomenon of wind self-oscillations caused by the nature of the laminar wind flow around the pipe is often found. At certain Reynolds numbers, on the leeward side of the pipe, the so-called Karman's track [1] is formed, consisting of vortices alternately breaking off from the upper and lower sides of the cylindrical surface of the pipe. These vortices transmit to the pipeline significant in magnitude sign-alternating pulses, which cause oscillations in the vertical plane, the frequency of which is equal to the vortex separation frequency. If this frequency coincides with the frequency of natural vibrations of the gas line, a resonance will occur, representing a serious danger to any structure. A rapid increase in the amplitude of vibrations leads to various damages: loosening of the supports, destruction of clamps at the points of attachment of the pipe with supports, the appearance of longitudinal and transverse cracks on the surface of the pipe at the support points, dropping the gas pipeline from the supports, etc.

The main conditions for the occurrence of wind self-oscillations are the laminar nature of the wind flow, the exclusion of local turbulence and the relatively high flexibility of the pipeline. It is known that for pipelines of medium (300-500 mm) and large (over 500 mm) diameters, the occurrence of wind self-oscillations is practically excluded, but for pipelines of smaller diameter this phenomenon can be destructive [2].

The existing methods for solving this problem are divided into two directions: changing the nature of the flow around a structure or the nature of the oscillatory process (active methods) and constructive limitation of the level of oscillations by changing the frequency of natural oscillations (passive) [3]. Active aerodynamic methods use various devices to change the nature of the flow around the structure (turbulators, perforated casings, etc.). Active mechanical dampers change dynamic characteristics without changing static ones (dampers, shock absorbers, etc.). Currently, active research is being conducted in both directions, but aerodynamic methods are more widespread.

Various methods of calculating systems with vibration damping devices are known in the literature [3, 4]. The article [5] examines the existing methods of calculating cylindrical structures for wind vibrations with mechanical damping devices.

In works [6, 7], the authors have studied the devices for active aerodynamic damping of wind self-oscillations of cylindrical structures. The obtained results of experiments in a wind tunnel show high efficiency of the devices. Similar studies are carried out by methods of numerical simulation [8]. In this case, in the formulation of problems, usually design dynamic models with a small number of degrees of freedom are considered, in which the internal friction of the material is taken into account on the basis of proportional damping models [9, 10].

This article analyzes the dynamic response of the gas pipeline design model in a non-stationary process. To limit the resonance amplitudes in the design model, a device is used that operates on the principle of one-way connection (OWC) and contains a cable with a zero bending stiffness as the main element [11]. Within the framework of the theory of temporal analysis, a mathematical model of oscillations of a system with one and two OWC is built. This model makes it possible to take into account the behavior of the system, both in the state of the base model (BM), when the OWC is turned off from work, and in the state of models with additional connection (MAC), when the OWC is turned on.

When analyzing the fluctuations of the design model, the influence of a number of factors on the parameters of the dynamic response of the design model was studied. In particular, the influence of the cable stiffness and the influence of the OWC location in the span relative to the supports were taken into account.

1. MODELS AND ALGORITHMS

The equation of motion of an elastic discrete dissipative system (DDS) in the framework of the linear model of viscous resistance (1) and the initial conditions (2) of the dynamic problem are represented in the form:

$$M\ddot{Y}(t)+C\dot{Y}(t)+KY(t)=P(t) \tag{1}$$

$$Y_0=Y(t_i)\,,\ \dot{Y}_0=\dot{Y}(t_i)\,, \tag{2}$$

where $M = \mathrm{diag}\,(m_1, ..., m_n)$, $C_j = C_j^{\mathrm{T}}$, $K_j = K_j^{\mathrm{T}} \in M_n(\mathrm{R})$ − mass matrix, damping matrix and stiffness matrix; $Y(t)$, $P(t)$ − displacement vectors and external load vectors. The index $j = 0, 1, \ldots$ takes into account the state of the design model over the time interval $t \in [t_i, t_{i+1}]$, at that, the zero index j of the corresponding matrices is omitted. Here t_i – is the OWC on / off time.

The construction of fundamental solutions of the homogeneous differential equation following from (1) is related to the matrix function $\Phi_j(t) = e^{S_j t}$ in which $S_j \in M_n(\mathrm{C})$ satisfies the characteristic matrix quadratic equation (MQE) – the equation of motion of natural forms:

$$MS_j^2+C_jS_j+K_j=0\,. \tag{3}$$

The matrices S_j play an exceptional role in the analysis of a dynamic system, because the spectra of these matrices contain the internal dynamic characteristics of the DDS (damping coefficients, frequencies and forms of natural vibrations). The MQE solution (3) has an analytical representation in the form of a root pair:

$$S_{j(1,2)}=M^{-1}(-C_j+V_j\pm U_j)/2 \tag{3}$$

where $V_j = -V_j^{\mathrm{T}}$, $U_j = U_j^{\mathrm{T}}$ – skew-symmetric and symmetric matrices.

For an elastic DDS with low dissipation, the elements of the matrices V_j, U_j are real and imaginary, respectively, and therefore the matrix roots $S_{j(1,2)}$ are complex conjugate ($S_{j,1} = S_j$, $S_{j,2} = \overline{S}_j$) [12]:

$$\begin{aligned} S_j&=M^{-1}(-C_j+V_j+U_j)/2\,,\\ \overline{S}_j&=M^{-1}(-C_j+V_j-U_j)/2\,. \end{aligned} \tag{4}$$

The system response (vectors of displacements and velocities of DDS nodes) is written in the matrix form of the Duhamel integral [13]:

$$Y(t)=2\,\mathrm{Re}\{Z(t)\}\,,\ \dot{Y}(t)=2\,\mathrm{Re}\{S_jZ(t)\}\,, \tag{5}$$

$$\begin{aligned} Z(t)&=\Phi_j(t-t_i)U_j^{-1}M(-\overline{S}_jY_0+\dot{Y}_0)+\\ &+U_j^{-1}\int_{t_i}^{t}\Phi_j(t-\tau)^{\mathrm{T}}P(\tau)d\tau. \end{aligned} \tag{6}$$

The first term in (6) expresses the reaction of the design model with free vibrations, the second term is the Duhamel integral, the reaction with forced vibrations.

The aerodynamic effect of the wind load is determined by the sine law:

$$P(t)=P_0\sin(\theta t)\,. \tag{7}$$

The amplitude value of the disturbing load acting in the node is calculated as the force of the frontal resistance to the static action of the wind of the calculated speed. The number of vortices escaping from the pipe surface in 2π seconds is the circular frequency of the disturbing load and is calculated using the following formula:

$$\theta=\frac{0,2v}{d}\cdot 2\pi\,. \tag{7}$$

Then the dynamic reaction (6) under the condition of constant velocity head (θ = const along the entire length of the design model) takes the form on the interval $t \in [t_i, t_{i+1}]$ [12]:

$$\left.\begin{aligned} Z(t)&=\Phi_j(t-t_i)U_j^{-1}M[-\overline{S}_jY_0+\dot{Y}_0]+\\ &+U_j^{-1}\left[(S_j^{\mathrm{T}})^2+\theta^2\right]^{-1}F(t)P_0,\\ F(t)&=S_j^{\mathrm{T}}\left[\Phi_j(t-t_i)^{\mathrm{T}}\sin(\theta t_i)-E\sin(\theta t_i)\right]+\\ &+\left[\Phi_j(t-t_i)^{\mathrm{T}}\cos(\theta t_i)-E\cos(\theta t_i)\right]\theta, \end{aligned}\right\} \tag{8}$$

where E – identity matrix.

The design scheme (Fig. 1) of the gas pipeline has the form of a continuous beam, all spans of which (except for the central one) are modeled by the same number of nodes containing point masses. In the central span, the number of nodes has been increased in order to improve the positioning accuracy of the OWC. The number of degrees of freedom of the system is equal to the number of masses.

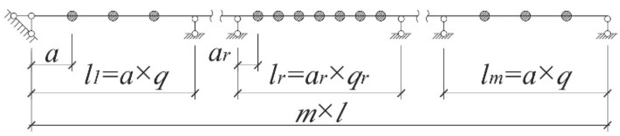

Figure 1. Design model

Activation and deactivation of connections is realized by changing the external (C_j, K_j) and internal (S_j, U_j) dynamic parameters of the system and changing the initial conditions (Y_0, $\dot{Y}_0$). In addition, when moving from interval $t \in [t_{i-1}, t_i]$ to interval $t \in [t_i, t_{i+1}]$, the time is changed from t_{i-1} to t_i.

In the case of a design dynamic model with one OWC in a span (DDM-1), Fig. 2 shows two possible states of the system (for $j = 0, 1$): BM and MAC. For a model with two OWC in a span (DDM-2), four possible states are considered ($j = 0, 1, 2, 3$): BM, MAC-1, MAC-2 and MAC-3 (Fig. 3).

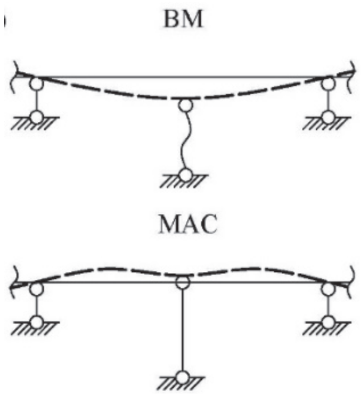

Figure 2. Schemes of possible states of the design model with one OWC (DDM-1)

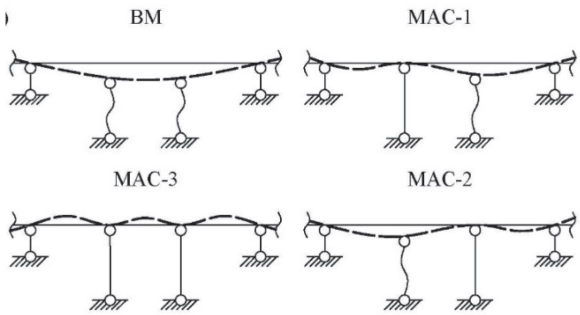

Figure 3. Schemes of possible states of the design model with two OWC (DDM-2)

Variants of the MAC-1, MAC-2 models (within the framework of the DDM-2) are possible with an arbitrary arrangement of the OWC in the central span and a velocity flow that is not constant along the length of the design model.

Initial data for calculation: outer and inner diameters of the pipe, respectively D = 219 мм, d = 209 мм, elastic modulus $E = 2{,}1 \times 10^8$ kN/m^2, span length l = 15 m, number of spans m = 9, the number of elementary sections in the central span q_1 = 16, in other spans q = 4. Accordingly, the number of masses in the central span is 15, in other spans – 3, the number of degrees of freedom n = 39. The tensile compliance of the cable takes values in the range $\delta_R \in [0.001, 0.1]$ m/kN. Logarithmic decrement δ = 0,07. The wind speed at which the resonance occurs is v = 2.951 m/s.

2. EXPERIMENTAL STUDIES OF THE "BEAM - CABLE" MODEL

Note that in Fig. 2, 3 show schemes of possible states of the system during vibrations only with a symmetrical arrangement of the deformed axis of the design model relative to the attachment point of the working (active) OWC, i.e. displacements of the elastic line when passing through the attachment point, where the OWC entered into operation, do not change sign. This is due to the fact that in the transient modes of the design model, when the BM is in one (any) of the states associated with the MAC, the stay in this state, as experimental studies show, lasts a fraction of a second and does not exceed 1/10 of the time the system is in condition BM.

The experiment was carried out on a flexible beam with one OWC. The aerodynamic effect was simulated using a vibration load from a light electric motor located in the center of the beam (Fig. 4). The parameters of the design dynamic model: the cross-section of the beam is 50 × 4 mm, the length is 2 m, one-way connection in the form of a cable, within the framework of the experiment, is assumed to be inextensible. Motor weight 0.36 kg, motor angular frequency causing resonance θ = 9 rad/s, amplitude of the active component of the vertical centrifugal force P_0 = 5.3 kg. The purpose of the experiment: to determine the form of vibration of the deformed axis of the beam at the moment of activation of the OWC (cable); to show that the form of natural vibrations of the model in the MAC state is symmetric due to the absence of turns of the central section at the point of attachment of the OWC to the beam.

In Fig. 4 shows a photo of the experimental setup at the moment of OWC tension (a) and OWC deactivation (b). In both Figures, it can be seen that the elastic line of the beam at the point of attachment of the cable retains its symmetry about the center of the span, and the tangent to the elastic line at this point does not rotate relative to the horizontal. It can be stated that due to the inertia of motion and because of the short duration of the stay of the design model in the MAC state, the model does not have time to change the type of symmetry of the form of natural vibrations.

Figure 5 shows the frequency characteristics of the vibrations of the BM (Fig.5a) and the model with a cable (Fig.5b), recorded using a special application «Vibration analysis». The vibration frequency of the BM is 1.62 Hz, the maximum value of the vibration displacement amplitude is 62.94 mm – 6.06 mm/s^2. The vibration frequency of the model with a cable is 4.94 Hz, the amplitude of vibration displacements is 2.27 mm, amplitude of accelerations is 23.59 mm/s^2.

a)

b)

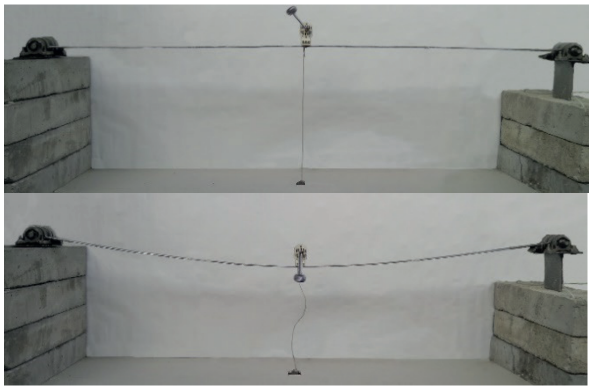

Figure 4. Design model "beam – cable": a – in a state of tension on the cable; b – when the cable is off

a)

b)

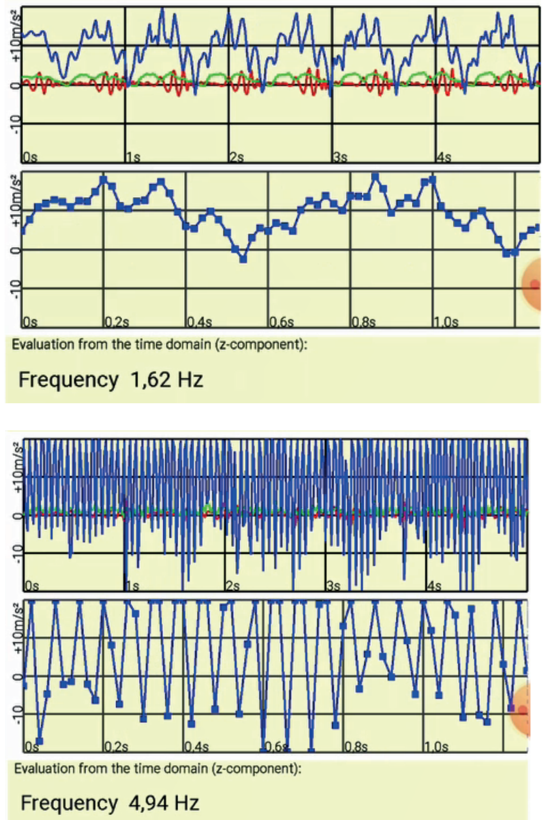

Figure 5. Characteristics of system oscillations: a) BM; b) model with a cable

It is important to note that when the beam is deformed in symmetric mode of vibration (Fig. 2, state of MAC-1), its displacements will be less than the corresponding displacements of the beam in the case of its deformation along the skew-symmetric mode of vibration. This is due to the fact that the central section of the beam in the MAC-1 state corresponds to the design scheme with a rigidly fixed support, and when deformed according to a skew-symmetric vibration mode, it corresponds to the design scheme with a hinged support.

Turning to the design model of a gas pipeline in the form of a multi-span beam, we can conclude that the use of a symmetric vibration mode reduces deflections not only in the central span where the OWC is installed, but also in adjacent spans of the design model. Here, the gas pipeline design behaves like a living organism, showing the "instinct of self-preservation" and choosing the most optimal way out of a critical situation. Indeed, in order to resist the wind resonance, the gas pipeline construct makes the most of its external and internal reserves. The OWC acts as an external reserve, the activation of which leads to a change in the calculation scheme, and the internal reserve is the symmetric form of the system's oscillations in a new state. This transformation of the system provides more effective resistance to wind resonance than in a system with a skew-symmetric vibration mode.

3. RESULTS OF THE STUDY

In the case of a design model with two OWC in a span (DDM-2), their symmetrical arrangement relative to the center of the span at the attachment points is considered: 19-21, 18-22 and 17-23 (Fig. 6). The results of computer simulation of the problem are graphs (oscillograms) of the parameters of the dynamic reaction of a constructively nonlinear dissipative system at a given time interval. These parameters include: displacement, velocity, acceleration, restoring (elastic), dissipative and inertial forces calculated in the design sections of the model, as well as the forces in the cables. The most indicative is the graph in which the kinematic and power parameters are combined. Figure 7 shows a fragment of an oscillogram of displacements, restoring forces and forces in the cable, built for the 19th node, where the left OWC is mounted in the DDM-2 (19-21) system. As can be seen from the graph, on time intervals corresponding to the OWC tension, displacements $y_{19}(t)$ of this node (due to the compliance of the connection) become higher than the position of static equilibrium. At this moment, the activation of elastic forces occurs due to a sharp transformation of kinetic energy into potential.

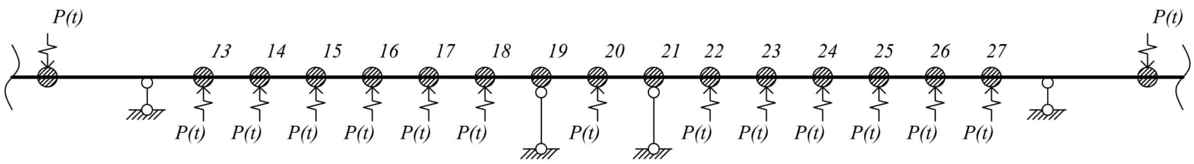

Figure 6. Scheme of application of loads in the central span of DDM-2 (19-21)

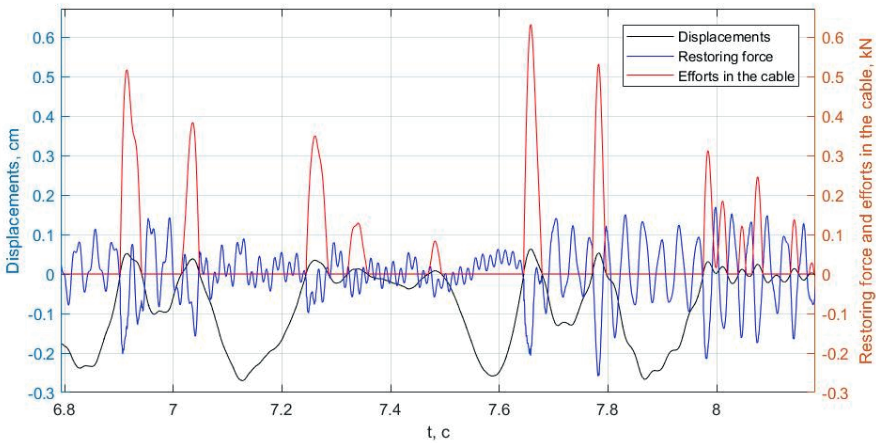

Figure 7. Fragment of the oscillogram of displacements, restoring force and efforts in the cable at the attachment point of the left OWC

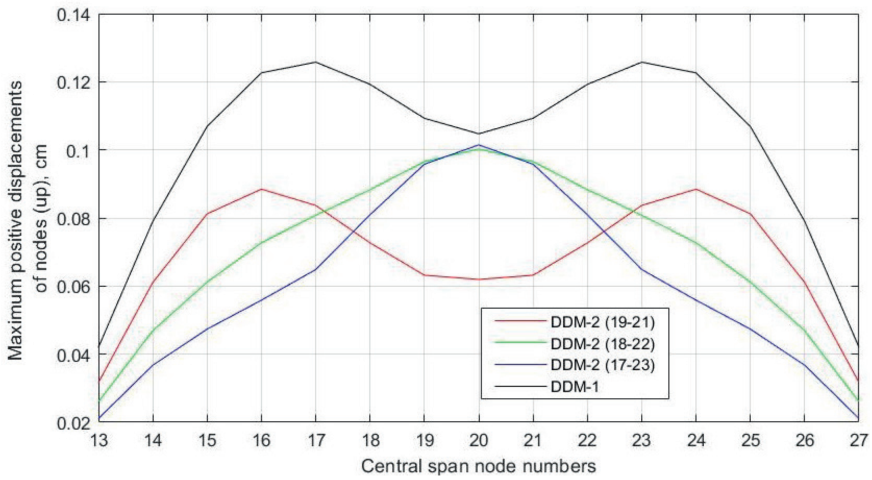

Figure 8. Graph of the maximum positive vibration displacements of the nodes of the central span

To compare the effectiveness of the ways of positioning the OWC in the span, a comparative calculation of DDM-1 and DDM-2 was carried out with the minimum cable complience (0.001 m / kN). The maximum developed displacements of the masses of the central span were estimated for the entire period of oscillations, for which the graphs of the maximum positive (upward) displacements were constructed, which, in fact, represent the enveloping diagrams of displacements (Fig. 8). The resulting graph shows that the level of fluctuations of the central span is most effectively suppressed in the DDM-2 with the OWC 19-21 location, that is, the closest to the center.

Fig. 9 shows oscillograms of the maximum displacements of the base model, DDM-1 and DDM-2 (19-21) with a cable compliance of 0.01 m/kN at a 10-second interval. As can be seen from the graph, in DDM-2 the maximum displacement values are less than in DDM-1, and the maximum is also reached earlier. Moreover, at the beginning of the process, the displacement in both models is higher than in the BM.

The maximum displacements develop at the central points of the extreme spans. Oscillograms of vibration displacements of DDM-1 and DDM-2 (19-21) for these points are shown in Fig. 10.

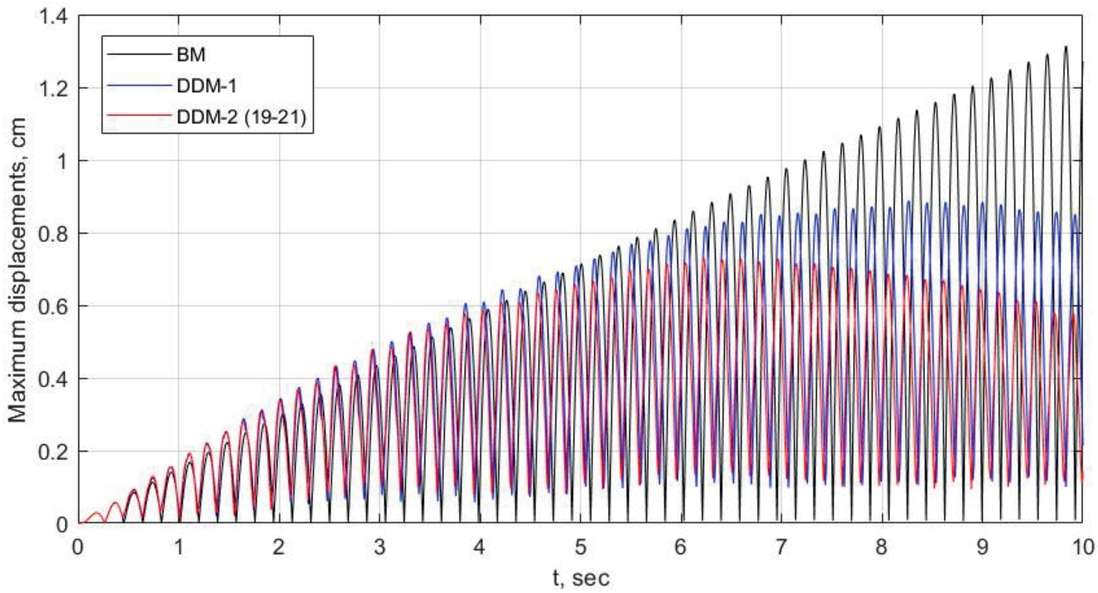

Figure 9. Oscillograms of maximum modulus displacements BM, DDM-1, DDM-2 (19-21)

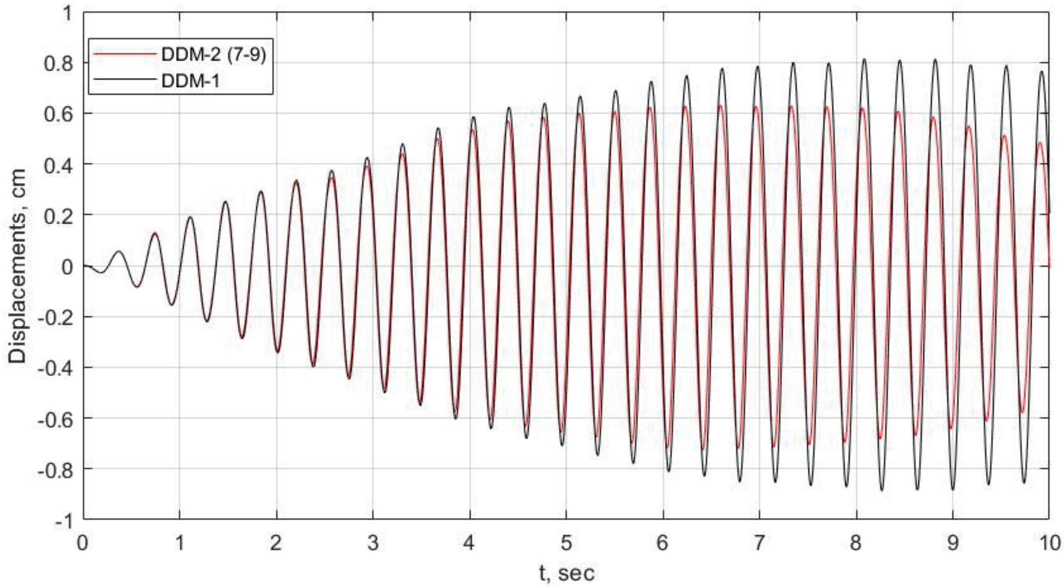

Figure 10. Oscillograms of movements of the central node of extreme span in DDM-1 and DDM-2 (19-21)

Fig. 11 shows a graph of the maximum vibration displacements max| $y_i(t)$ | for models DDM-1, DDM-2 at different values of cable compliance (from 0.001 to 0.1 m/kN).

According to the graph, the DDM-2 model (19-21) shows the maximum efficiency in almost the entire range of cable compliance values. The variant with the DDM-1 model shows the worst results in all cases. Moreover, a twofold increase in the rigidity (decrease in compliance) of the cable in DDM-1 does not give an advantage over DDM-2 in the effective range of rigidity (compliance range from 10^{-3} to $5 \cdot 10^{-2}$ m/kN). In other words, a single double-stiffness cable is not more efficient than two single-stiffness cable.

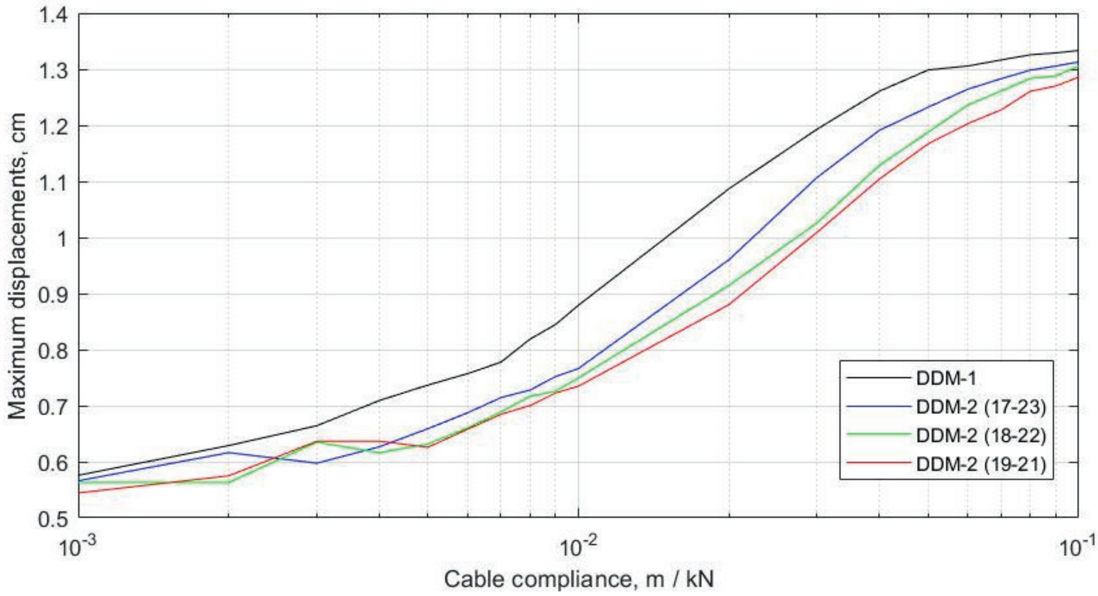

Figure 11. Graph of the dependence of the maximum vibration displacements on the cable compliance in various models

The phase diagrams $y_i(t) - \dot{y}_i(t)$ shown in Fig. 12, built for the case of the lowest cable compliance (0,001 м/кН) in the first two seconds of the system operation, demonstrate the differences in the nature of the nonlinear operation of the system. Here the *i* numbers correspond to the central nodes of the corresponding spans.

In BM, the phase trajectory of the central node of the 4th span is characterized by a uniform proportional increase in the form of a spiral. (Fig. 12 a). The same dependences constructed for DDM-1 and DDM-2 (Fig. 12 b, c), not only differ from BM, but also significantly differ from each other. For DDM-2, in comparison with DDM-1, sharper and more frequent changes in the direction of speed are characteristic, which is a reflection of the higher energy impact on the constructive nonlinear model from the side of the two OWCs when they are switched on / off. Phase diagrams of off-center (extreme) nodes of the 4th span have a similar look. In the first span operation character DDM-2 is aligned, it becomes more similar to the operation of BM (Fig. 12 g).

For the computational model with two OWC, an estimate of the accuracy of solving the differential equation of motion using the residual vector $\Delta\varphi(t) = f(t) - P(t)$, where $f(t) = M\ddot{Y}(t) + C\dot{Y}(t) + KY(t)$ is the sum of inertial, dissipative and restoring forces on the left side of the equation; $P(t) = [p_j(t)]$ – vector of external forces. Value $\Delta\varphi(t)$, expressing the difference between the left and right sides of the equation, is built for DDM-2 over the entire response interval, including the states of BM and MAC-2. The nature of the convergence of the solution (functions $f_j(t)$) to the given functions $p_j(t)$ of the right-hand side of the equation is shown on the oscillogram $\Delta\varphi_j(t)$ for the cable attachment point (j = 7) in Fig. 13. The accuracy of solving the differential equation of motion does not go beyond the error limits $\varepsilon \le 8{,}5\times10^{-13}$ кН.

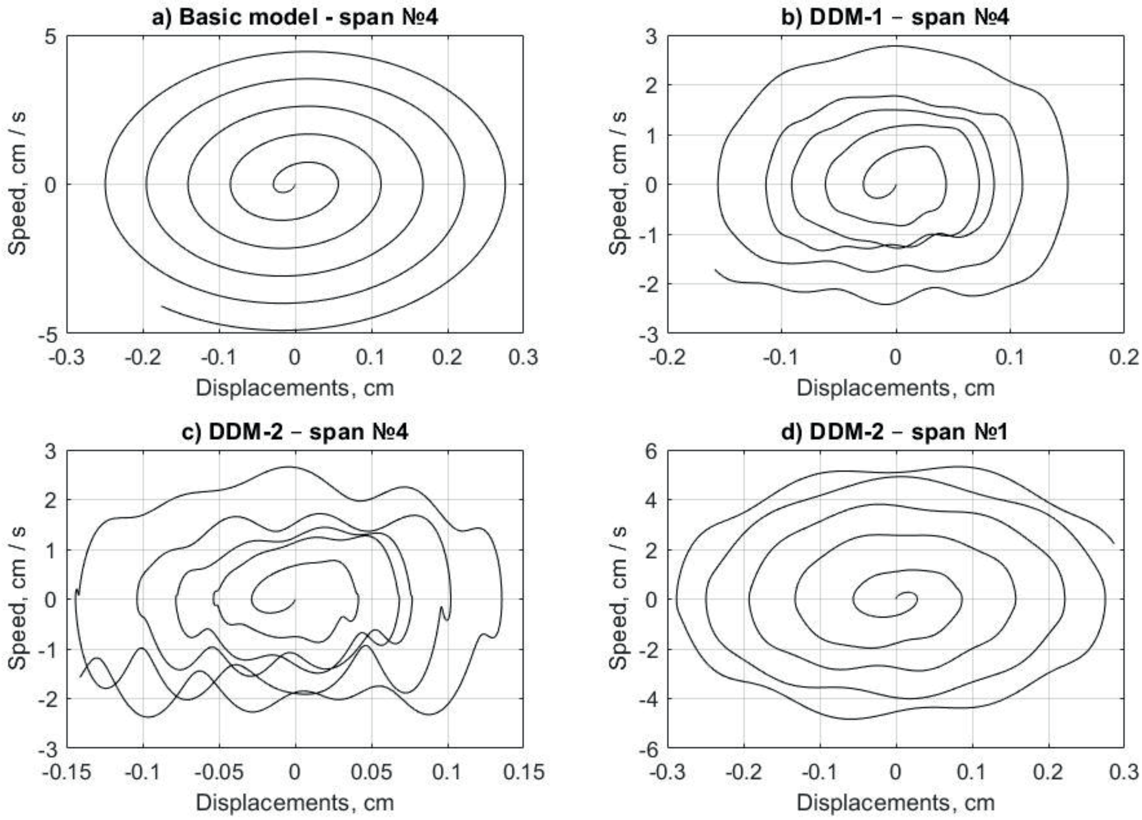

<u>Figure 12.</u> Phase trajectories in coordinates $y_i(t) - \dot{y}_i(t)$ for BM, DDM-1 and DDM-2 in the first two seconds of operation with cable compliance 0.001 m / kN

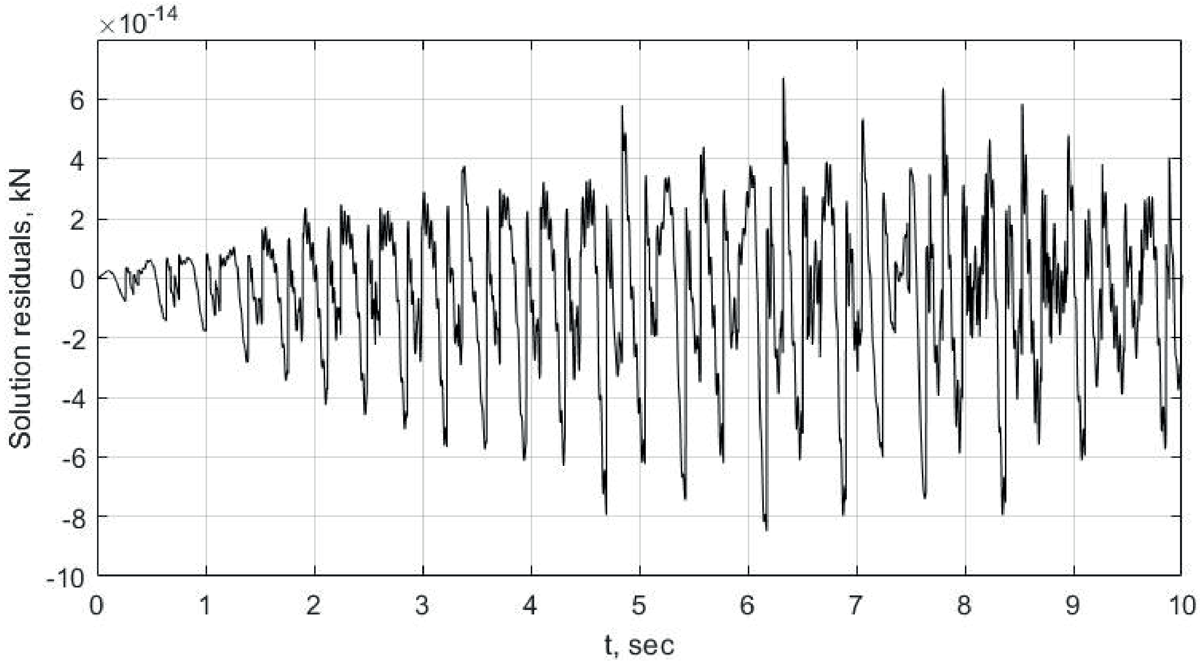

Figure 13. Oscillogram of residuals $\Delta\varphi_7(t)$ of the solution of the equation of motion (1)

CONCLUSION

Based on the results of the study, the following conclusions can be drawn.

1. On the basis of experimental data, a more perfect model with a symmetric natural vibration mode was adopted. Computer simulation of the problem with one and two OWC also showed a high efficiency of the damping device for the proposed oscillation model. This result is of great practical importance. The use of this model (within the framework of DDM-1 and DDM-2) will increase (optimize) the spacing of vibration damping devices along the elevated gas pipeline route and, thereby, reduce the number of these devices per one kilometer of the route compared to the model of vibrations with a skew-symmetric shape.
2. For DDM-2 with a symmetrical arrangement of the OWC, the optimal arrangement of connections (19-21 – in the local numbering of the central span) was obtained practically over the entire range of values of the cable compliance. With this arrangement of connections, the DDM-2 shows a more active limitation of the amplitudes of the parameters of the dynamic response in comparison with the same model with other arrangements of the OWC, and also in comparison with the DDM-1 model.
3. It is shown that all the considered variants of the DDM-2 models lead to much lower amplitudes of the response parameters in comparison with the DDM-1 model. Even a doubling of stiffness of the cable in the DDM-1 model did not reveal any advantages over the DDM-2 model in terms of maximum vibration displacements.

REFERENCES

1. **Bisplinghoff, R.L.** Aeroelasticity: monograph [Aerouprugost': monografiya] / R.L. Bisplinghoff, H. Eshli, R.L. Halfman. – Moscow.: IL, 1958. 799 p.
2. **Tartakovsky, G.A.** Pipeline structural mechanics [Stroitel'naya mekhanika truboprovoda] / G.A. Tartakovsky. -– Moscow.: «Nedra» Publ., 1967. 312 p.
3. **Kazakevich, M.I.** Aerodynamic stability of overground and overhead pipelines [Aerodinamicheskaya ustojchivost' nadzemnyh i visyachih truboprovodov] / M.I. Kazakevich. – Moscow.: «Nedra» Publ., 1977. 200 p.

4. Dynamic calculation of buildings and structures [Dinamicheskij raschet zdanij i sooruzhenij] / M.F. Bernshtejn, V.A. Il'ichev, B.G. Korenev [et al.]; edited by B.G. Korenev, I.M. Rabinovich. – 2-nd edition revised and enlarged – Moscow.: Strojizdat, 1984. – 303 p.
5. **Gabbai, R.D., Benaroya, H.** An overview of modeling and experiments of vortex-induced vibration of circular cylinders // Journal of Sound and Vibration. – 2005. – Vol. 282. – P. 575–616.
6. **Wen-Li Chen, Guan-Bin Chen, Feng Xu, Ye-wei Huang, Dong-Lai Gao, Hui Li.** Suppression of vortex-induced vibration of a circular cylinder by a passive-jet flow control // Journal of Wind Engineering & Industrial Aerodynamics. – 2020. – Vol. 199. P. – 1-13.
7. **Wang L., Jiang T.L., Dai H.L., Ni Q.** Three-dimensional vortex-induced vibrations of supported pipes conveying fluid based on wake oscillator models // Journal of Sound and Vibration. – 2018. – Vol. 422. – P. 590-612.
8. **Muddadaa S., Patnaik B.S.V.** Active flow control of vortex induced vibrations of a circular cylinder subjected to non-harmonic forcing // Ocean Engineering. – 2017. – Vol. 142. – P. 62-77.
9. **Lupi F., Niemann H-J., Hoffer R.** Aerodynamic damping model in vortex-induced vibrations for wind engineering applications // Journal of Wind Engineering & Industrial Aerodynamics. – 2018. – Vol. 174. – P. 281-295.
10. **Lei Wang, Xing-Yan Fan, Shu-Guo Liang, Jie Song, Ze-Kang Wang**. Improved expression for across-wind aerodynamic damping ratios of super high-rise buildings // Journal of Wind Engineering & Industrial Aerodynamics. – 2018. – Vol. 176. – P. 263-272.
11. Patent RF №2007109081/12.03.2007 Pipeline resonance damping device [Ustrojstvo dlya gasheniya rezonansnyh kolebanij truboprovoda] // Patent, Russia №66000.2019. Bulletin № 25. / Potapov A.N., Degtyareva N.V. [et al.].
12. **Potapov A.N.** Dynamic analysis of discrete dissipative systems under nonstationary influences [Dinamicheskij analiz diskretnyh dissipativnyh sistem pri nestacionarnyh vozdejstviyah] / A.N. Potapov. – Chelyabinsk: SUSU Publ., 2003. 167 p.
13. **Potapov, A.N.** Analysis of vibrations of structures with switching off connections [Analiz kolebanij konstrukcij s vyklyuchayushchimisya svyazyami] / A.N. Potapov // Bulletin of SUSU. Series: Construction and architecture. 2017. – Vol.17, №1. pp. 38-48. DOI: 10.14529/build170105

СПИСОК ЛИТЕРАТУРЫ

1. **Бисплингхофф, Р.Л.** Аэроупругость: монография / Р.Л. Бисплингхофф, Х. Эшли, Р.Л. Халфман. – М.: ИЛ, 1958. – 799 с.
2. **Тартаковский, Г.А.** Строительная механика трубопровода / Г. А. Тартаковский. - М.: «Недра», 1967. – 312 с.
3. **Казакевич, М.И.** Аэродинамическая устойчивость надземных и висячих трубопроводов / М.И. Казакевич. – М.: «Недра», 1977. – 200 с.
4. Динамический расчет зданий и сооружений / М.Ф. Бернштейн, В.А. Ильичев, Б.Г. Коренев [и др.]; под ред. Б.Г. Коренева, И.М. Рабиновича. – 2-е изд., перераб. И доп. – М.: Стройиздат, 1984. – 303 с.
5. **Gabbai, R.D., Benaroya, H.** An overview of modeling and experiments of vortex-induced vibration of circular cylinders // Journal of Sound and Vibration. – 2005. – Vol. 282. – P. 575–616.
6. **Wen-Li Chen, Guan-Bin Chen, Feng Xu, Ye-wei Huang, Dong-Lai Gao, Hui Li**. Suppression of vortex-induced vibration of a circular cylinder by a passive-jet flow control // Journal of Wind Engineering & Industrial Aerodynamics. – 2020. – Vol. 199. P. – 1-13.

7. **Wang L., Jiang T.L., Dai H.L., Ni Q**. Three-dimensional vortex-induced vibrations of supported pipes conveying fluid based on wake oscillator models // Journal of Sound and Vibration. – 2018. – Vol. 422. – P. 590-612.
8. **Muddadaa S., Patnaik B.S.V**. Active flow control of vortex induced vibrations of a circular cylinder subjected to non-harmonic forcing // Ocean Engineering. – 2017. – Vol. 142. – P. 62-77.
9. **Lupi F., Niemann H-J., Hoffer R.** Aerodynamic damping model in vortex-induced vibrations for wind engineering applications // Journal of Wind Engineering & Industrial Aerodynamics. – 2018. – Vol. 174. – P. 281-295.
10. **Lei Wang, Xing-Yan Fan, Shu-Guo Liang, Jie Song, Ze-Kang Wang**. Improved expression for across-wind aerodynamic damping ratios of super high-rise buildings // Journal of Wind Engineering & Industrial Aerodynamics. – 2018. – Vol. 176. – P. 263-272.
11. Патент РФ №2007109081/ 12.03.2007 Устройство для гашения резонансных колебаний трубопровода // Патент России №66000.2019. Бюл. № 25. / Потапов А.Н., Дегтярева Н.В. [и др.].
12. **Потапов А.Н.** Динамический анализ искретных диссипативных систем при нестационарных воздействиях / А.Н. Потапов. – Челябинск: Изд-во ЮУр-ГУ, 2003. – 167 с.
13. **Потапов, А.Н.** Анализ колебаний конструкций с выключающимися связями / А.Н. Потапов // Вестник ЮУрГУ. Серия «Строительство и архитектура». – 2017. – Т. 17, № 1. – С. 38–48. DOI: 10.14529/build170105

Alexander N. Potapov, South-Ural State University (National Research University), Department of Building Technologies and Structural Engineering, Doctor of Technical Sciences, Professor of the Department, Professor, Corresponding Member RAASN, 76, Lenin Prospect, Chelyabinsk, 454080, Russia. phone: +7(351)267-91-83, 8-9193437129. E-mail: potapov.alni@gmail.com.

Nail T. Tazeev, South-Ural State University (National Research University), Department of Building Technologies and Structural Engineering, graduate student, 76, Lenin Prospect, Chelyabinsk, 454080, Russia. phone: 8-951-253-16-85. E-mail: tazeev.nail@gmail.com

Потапов Александр Николаевич, ФГАОУ ВО «Южно-Уральский государственный университет» (Национальный исследовательский университет), кафедра «Строительное производство и теория сооружений», д.т.н., проф. каф., профессор, член-корреспондент РААСН, 454080, Россия, г. Челябинск, пр. Ленина, дом 76, тел.: +7(351) 267-91-83, 8-9193437129. E-mail: potapov.alni@gmail.com.

Тазеев Наиль Тимурович, ФГАОУ ВО «Южно-Уральский государственный университет» (НИУ), кафедра «Строительное производство и теория сооружений», аспирант, 454080, Россия, г. Челябинск, пр. Ленина, дом 76, тел.: 8-951-253-16-85. E-mail: tazeev.nail@gmail.com